20 The Hadley Circulation and the ITCZ

20.1 Introduction

When an east-west line of deep convection forms near the equator, it begins to change the potential vorticity field due to latent heat release. In the Northern Hemisphere such convection induces a positive potential vorticity anomaly at low levels and a negative anomaly aloft. Since this convectively induced potential vorticity anomaly develops from an initial state which has potential vorticity increasing toward the north, reversed poleward gradients of potential vorticity tend to be produced. The regions of potential vorticity gradient reversal are expected to be found on the poleward side of the ITCZ at low levels and on the equatorward side of the ITCZ at upper levels. This sets the stage for combined barotropic-baroclinic instability, the formation of tropical waves, and the breakdown of the ITCZ. The use of potential vorticity arguments seems the most direct way of understanding this process.

20.2 Derivation of the zonal mean equations

We consider a compressible, stably stratified, quasi-static atmosphere on the sphere. Using potential temperature θ as the vertical coordinate, using spherical coordinates in the horizontal, and denoting the zonal wind by u and the meridional wind by v, the governing set of primitive equations takes the form

$$\frac{\partial u}{\partial t} + \dot{\theta}\frac{\partial u}{\partial \theta} - \sigma P v + \frac{\partial}{a\cos\phi\partial\lambda}\left[M + \tfrac{1}{2}(u^2+v^2)\right] = F, \tag{20.1}$$

$$\frac{\partial v}{\partial t} + \dot{\theta}\frac{\partial v}{\partial \theta} + \sigma P u + \frac{\partial}{a\partial\phi}\left[M + \tfrac{1}{2}(u^2+v^2)\right] = G, \tag{20.2}$$

$$\frac{\partial M}{\partial \theta} - \Pi = 0, \tag{20.3}$$

$$\frac{\partial \sigma}{\partial t} + \frac{\partial(\sigma u)}{a\cos\phi\partial\lambda} + \frac{\partial(\sigma v\cos\phi)}{a\cos\phi\partial\phi} + \frac{\partial(\sigma\dot{\theta})}{\partial\theta} = 0, \tag{20.4}$$

where $\sigma = -\partial p/\partial\theta$ is the pseudodensity, $\Pi = c_p(p/p_0)^\kappa$ the Exner function, $P = \zeta_\theta/\sigma$ the potential vorticity, $\zeta_\theta = 2\Omega\sin\phi + \partial v/a\cos\phi\partial\lambda - \partial(u\cos\phi)/a\cos\phi\partial\phi$ the isentropic absolute vorticity, $M = \theta\Pi + gz$ the Montgomery potential, and F, G the zonal and meridional components of the frictional force per unit mass. Expressing σ and Π in terms of p, we can regard (20.1)–(20.4) as a closed system in u, v, M and p. We do not regard $F, G, \dot{\theta}$ as unknown, but rather as given in terms of the known or parameterized momentum and heat sources/sinks. Of course, for adiabatic flow $\dot{\theta} = 0$.

To derive the zonal mean equations from (20.1)–(20.4) we shall define two types of zonal average—an ordinary zonal average on an isentropic surface and a mass weighted zonal average on an isentropic surface. For example, for the zonal wind u, the ordinary zonal average is defined by

$$\bar{u}(\phi,\theta,t) = \frac{1}{2\pi}\int_0^{2\pi} u(\lambda,\phi,\theta,t)\,d\lambda. \tag{20.5}$$

For the meridional wind v, the mass weighted zonal average is defined by

$$\hat{v} = \frac{\overline{\sigma v}}{\bar{\sigma}}. \tag{20.6}$$

Deviations from the ordinary zonal average of u are defined by $u' = u - \bar{u}$ and deviations from the mass weighted zonal average of v by $v^* = v - \hat{v}$. Similar definitions hold for the other variables.

Applying $\overline{(\ )}$ to each term in (20.4) and noting from (20.6) that $\overline{\sigma v} = \bar{\sigma}\hat{v}$ and $\overline{\sigma\dot{\theta}} = \bar{\sigma}\hat{\dot{\theta}}$, we can write the zonal mean mass continuity equation as

$$\frac{\partial\bar{\sigma}}{\partial t} + \frac{\partial(\bar{\sigma}\hat{v}\cos\phi)}{a\cos\phi\partial\phi} + \frac{\partial(\bar{\sigma}\hat{\dot{\theta}})}{\partial\theta} = 0. \tag{20.7}$$

This equation can also be written in the advective form (20.15).

To derive the equation for the mean zonal motion we first apply the $\overline{(\ )}$ operator to each term in (20.1), which yields

$$\frac{\partial \bar{u}}{\partial t} + \overline{\dot{\theta}\frac{\partial u}{\partial \theta}} - \overline{\sigma P v} = \bar{F}. \tag{20.8}$$

Noting that $\dot{\theta} = \hat{\dot{\theta}} + \dot{\theta}^*$, $P = \hat{P} + P^*$ and $v = \hat{v} + v^*$, we can write $\overline{\dot{\theta}\partial u/\partial\theta} = \hat{\dot{\theta}}\partial\bar{u}/\partial\theta + \overline{\dot{\theta}^*\partial u/\partial\theta}$ and $\overline{\sigma P v} = \bar{\sigma}\hat{P}\hat{v} + \overline{\sigma P^* v^*}$ since $\overline{\sigma v^*} = 0$ and $\overline{\sigma P^*} = 0$. Thus, (20.8) can be written

$$\frac{\partial \bar{u}}{\partial t} + \hat{\dot{\theta}}\frac{\partial \bar{u}}{\partial \theta} - \bar{\sigma}\hat{P}\hat{v} = \mathcal{F}, \tag{20.9}$$

where $\mathcal{F}$ is defined below in (20.17). Noting that $a\mathcal{D}\phi/\mathcal{D}t = \hat{v}$ (easily confirmed by applying (20.16) to ϕ) and that $\bar{\sigma}\hat{P} = \bar{\zeta}_\theta = 2\Omega\sin\phi - \partial(\bar{u}\cos\phi)/a\cos\phi\partial\phi$, (20.9) can be written in the absolute angular momentum form given below in (20.12).

Now consider the meridional momentum equation. Since both (20.12) and (20.15) contain $\hat{v}$, we would like to transform (20.2) into a prediction equation for $\hat{v}$. This requires putting (20.2) into a flux form before taking the zonal average. Thus, combining (20.2) and (20.4), we obtain the flux form

$$\frac{\partial(\sigma v)}{\partial t} + \frac{\partial(\sigma u v)}{a\cos\phi\partial\lambda} + \frac{\partial(\sigma v v\cos\phi)}{a\cos\phi\partial\phi} + \frac{\partial(\sigma\dot{\theta}v)}{\partial\theta} + \left(2\Omega\sin\phi + \frac{u\tan\phi}{a}\right)\sigma u + \sigma\frac{\partial M}{a\partial\phi} = \sigma G. \tag{20.10}$$

Taking the zonal average of (20.10), we obtain

$$\frac{\partial(\overline{\sigma v})}{\partial t} + \frac{\partial(\overline{\sigma v v}\cos\phi)}{a\cos\phi\partial\phi} + \frac{\partial(\overline{\sigma\dot{\theta}v})}{\partial\theta} + \overline{\left(2\Omega\sin\phi + \frac{u\tan\phi}{a}\right)\sigma u} + \overline{\sigma\frac{\partial M}{a\partial\phi}} = \overline{\sigma G}. \tag{20.11}$$

Noting that $\overline{\sigma v} = \bar{\sigma}\hat{v}$, $\overline{\sigma G} = \bar{\sigma}\hat{G}$, $\overline{\sigma v v} = \bar{\sigma}\hat{v}\hat{v} + \overline{\sigma v^* v^*}$, $\overline{\sigma\dot{\theta}v} = \bar{\sigma}\hat{\dot{\theta}}\hat{v} + \overline{\sigma\dot{\theta}^* v^*}$, $\overline{\sigma\partial M/a\partial\phi} = \bar{\sigma}\partial\bar{M}/a\partial\phi + \overline{\sigma'\partial M'/a\partial\phi}$, and using the zonal mean continuity equation (20.7), we obtain the advective form (20.13).

Collecting the above results, and taking the zonal average of (20.3), we obtain the complete set of zonal mean flow equations

$$\frac{\mathcal{D}(\bar{u}\cos\phi + \Omega a\cos^2\phi)}{\mathcal{D}t} = \mathcal{F}\cos\phi, \tag{20.12}$$

$$\frac{\mathcal{D}\hat{v}}{\mathcal{D}t} + \left(2\Omega\sin\phi + \frac{\bar{u}\tan\phi}{a}\right)\bar{u} + \frac{\partial\bar{M}}{a\partial\phi} = \mathcal{G}, \tag{20.13}$$

$$\frac{\partial\bar{M}}{\partial\theta} - \Pi(\bar{p}) = \overline{\Pi(p)} - \Pi(\bar{p}), \tag{20.14}$$

$$\frac{\mathcal{D}\bar{\sigma}}{\mathcal{D}t} + \bar{\sigma}\left(\frac{\partial(\hat{v}\cos\phi)}{a\cos\phi\partial\phi} + \frac{\partial\hat{\dot{\theta}}}{\partial\theta}\right) = 0, \tag{20.15}$$

where

$$\frac{\mathcal{D}}{\mathcal{D}t} = \frac{\partial}{\partial t} + \hat{v}\frac{\partial}{a\partial\phi} + \hat{\dot{\theta}}\frac{\partial}{\partial\theta} \tag{20.16}$$

is the derivative following the mass weighted mean meridional circulation, and

$$\mathcal{F} = \bar{F} + \overline{\sigma P^* v^*} - \overline{\dot{\theta}^*\frac{\partial u}{\partial\theta}}, \tag{20.17}$$

$$\mathcal{G} = \hat{G} - \frac{1}{\bar{\sigma}}\left[\frac{\partial\left(\overline{\sigma v^* v^*}\cos\phi\right)}{a\cos\phi\partial\phi} + \frac{\partial\left(\overline{\sigma\dot{\theta}^* v^*}\right)}{\partial\theta} + \left(2\Omega\sin\phi + \frac{\bar{u}\tan\phi}{a}\right)\overline{\sigma' u'} + \frac{\overline{(\sigma u)' u'}\tan\phi}{a} + \overline{\sigma'\frac{\partial M'}{a\partial\phi}}\right], \tag{20.18}$$

are the eddy-induced effective mean zonal and meridional forces per unit mass. Equations (20.12)–(20.15) have the form of the zonally symmetric primitive equations for $\bar{u}$, $\hat{v}$, $\bar{M}$, $\bar{p}$, all of which are functions of (ϕ, θ, t). The terms $\mathcal{F}$, $\mathcal{G}$, $\hat{\dot{\theta}}$ appear as forcings. As discussed in Appendix I, it is possible to express the eddy-induced part of $\mathcal{F}$ in terms of the divergence (or, more generally, pseudodivergence) of the Eliassen-Palm flux. We shall not need such expressions here, since the compact form (20.17) is well-suited for such problems as understanding the interactions of symmetric and asymmetric components of the flow, e.g., the influence of tropical upper tropospheric troughs (TUTTs) on the mean circulation.

The governing equation for the mass weighted zonal mean potential vorticity $\hat{P}$ can be derived by first noting that the equation for the zonal mean absolute isentropic vorticity (derived from (20.9) or (20.12)) takes the form

$$\frac{\mathcal{D}\bar{\zeta}_\theta}{\mathcal{D}t} + \bar{\zeta}_\theta \left(\frac{\partial(\hat{v}\cos\phi)}{a\cos\phi\partial\phi} + \frac{\partial\hat{\dot{\theta}}}{\partial\theta} \right) = \frac{\partial\bar{u}}{\partial\theta}\frac{\partial\hat{\dot{\theta}}}{a\partial\phi} + \bar{\zeta}_\theta\frac{\partial\hat{\dot{\theta}}}{\partial\theta} - \frac{\partial(\mathcal{F}\cos\phi)}{a\cos\phi\partial\phi}. \tag{20.19}$$

Eliminating the isentropic divergence between (20.15) and (20.19) we obtain the mass weighted zonal mean potential vorticity equation

$$\bar{\sigma}\frac{\mathcal{D}\hat{P}}{\mathcal{D}t} = \frac{\partial\bar{u}}{\partial\theta}\frac{\partial\hat{\dot{\theta}}}{a\partial\phi} + \bar{\zeta}_\theta\frac{\partial\hat{\dot{\theta}}}{\partial\theta} - \frac{\partial(\mathcal{F}\cos\phi)}{a\cos\phi\partial\phi}, \tag{20.20}$$

where $\hat{P} = \bar{\zeta}_\theta/\bar{\sigma}$.

20.3 The potential latitude coordinate

A simple meridional coordinate transformation leads to a simplification of both the right hand side of (20.20) and the material derivative operator on the left hand side. To accomplish this transformation, let us now introduce the potential latitude Φ, defined in terms of the absolute angular momentum per unit mass by $\Omega a\cos^2\Phi = \bar{u}\cos\phi + \Omega a\cos^2\phi$. Consider $(\Phi, \Theta, \mathcal{T})$ space, where $\Theta = \theta$ and $\mathcal{T} = t$. The symbols Θ and $\mathcal{T}$ are introduced to distinguish partial derivatives at fixed Φ ($\partial/\partial\Theta$ and $\partial/\partial\mathcal{T}$) from partial derivatives at fixed ϕ ($\partial/\partial\theta$ and $\partial/\partial t$). Derivatives in (ϕ, θ, t) space are then related to derivatives in $(\Phi, \Theta, \mathcal{T})$ space by

$$\left(\frac{\partial}{\partial\phi}, \frac{\partial}{\partial\theta}, \frac{\partial}{\partial t} \right) = \left(\frac{\partial\Phi}{\partial\phi}\frac{\partial}{\partial\Phi}, \frac{\partial\Phi}{\partial\theta}\frac{\partial}{\partial\Phi} + \frac{\partial}{\partial\Theta}, \frac{\partial\Phi}{\partial t}\frac{\partial}{\partial\Phi} + \frac{\partial}{\partial\mathcal{T}} \right). \tag{20.21}$$

Another way of writing the first entry in (20.21) is $\partial/\cos\phi\partial\phi = (\bar{\zeta}_\theta/2\Omega\sin\Phi)\partial/\cos\Phi\partial\Phi$. Thus, in regions where $\bar{\zeta}_\theta > 2\Omega\sin\Phi$, the Φ coordinate provides a natural stretching which is analogous to the way the geostrophic coordinate provides stretching around fronts in semigeostrophic theory. To simplify the right hand side of (20.20), we now use (20.21) to obtain

$$\begin{aligned}
\frac{\partial\bar{u}}{\partial\theta}\frac{\partial\hat{\dot{\theta}}}{a\partial\phi} + \bar{\zeta}_\theta\frac{\partial\hat{\dot{\theta}}}{\partial\theta} - \frac{\partial(\mathcal{F}\cos\phi)}{a\cos\phi\partial\phi} &= 2\Omega\sin\Phi\frac{\partial(\sin\Phi, \hat{\dot{\theta}})}{\partial(\sin\phi, \theta)} - \frac{\partial(\mathcal{F}\cos\phi)}{a\cos\phi\partial\phi} \\
&= -\frac{\bar{\zeta}_\theta}{2\Omega\sin\Phi}\frac{\partial(\mathcal{F}\cos\phi)}{a\cos\Phi\partial\Phi} + 2\Omega\sin\Phi\frac{\partial(\sin\Phi, \Theta)}{\partial(\sin\phi, \theta)}\frac{\partial(\sin\Phi, \hat{\dot{\Theta}})}{\partial(\sin\Phi, \Theta)} \\
&= \bar{\zeta}_\theta\left(\frac{\partial(\hat{V}\cos\Phi\sin\Phi)}{a\cos\Phi\sin\Phi\partial\Phi} + \frac{\partial\hat{\dot{\Theta}}}{\partial\Theta} \right),
\end{aligned} \tag{20.22}$$

where $\hat{V} = a\mathcal{D}\Phi/\mathcal{D}t$ is given (using (20.12)) in terms of $\mathcal{F}$ by $-(2\Omega\sin\Phi)\hat{V}\cos\Phi = \mathcal{F}\cos\phi$, and where $\hat{\dot{\Theta}} = \hat{\dot{\theta}}$. Using (20.22) in (20.20) we obtain

$$\frac{\mathcal{D}\hat{P}}{\mathcal{D}t} = \hat{P}\left(\frac{\partial(\hat{V}\cos\Phi\sin\Phi)}{a\cos\Phi\sin\Phi\partial\Phi} + \frac{\partial\hat{\dot{\Theta}}}{\partial\Theta} \right). \tag{20.23}$$

The $\mathcal{D}/\mathcal{D}t$ operator, defined in (ϕ, θ, t)-space by (20.16), can also be expressed in $(\Phi, \Theta, \mathcal{T})$-space, since (20.21) can be used to show that

$$\frac{\mathcal{D}}{\mathcal{D}t} = \frac{\partial}{\partial\mathcal{T}} + \hat{V}\frac{\partial}{a\partial\Phi} + \hat{\dot{\Theta}}\frac{\partial}{\partial\Theta}. \tag{20.24}$$

In comparing (20.16) and (20.24) we note that the $(\Phi, \Theta, \mathcal{T})$-version of $\mathcal{D}/\mathcal{D}t$ is simpler than the (ϕ, θ, t)-version because the mass weighted mean meridional velocity $\hat{v}$ does not occur explicitly in (20.24). In the next section we shall see that this eliminates the need to solve a diagnostic equation for the meridional circulation in the $(\Phi, \Theta, \mathcal{T})$-version of balanced theory.

Note that $\hat{V}$ is the rate at which particles (in the mass weighted zonal mean sense) are crossing absolute angular momentum surfaces. In the upper levels of the Hadley circulation, the frictional effect $\bar{F}$ is negligible. Potential vorticity rearrangement due to TUTTs would usually appear to result in a equatorward eddy flux of PV, i.e., $\overline{\sigma P^* v^*} < 0$. Thus, from (20.17), we have $\mathcal{F} \approx \overline{\sigma P^* v^*} < 0$, so that $\hat{V} > 0$, i.e., particles are drifting northward across the zonal mean absolute angular momentum surfaces. An interesting question is whether the eddy-induced effective mean zonal force per unit mass $\overline{\sigma P^* v^*}$ can ever be of such a large magnitude that it plays as important a role as $\hat{\dot{\theta}}$ in shaping the Hadley circulation.

A concept closely related to potential vorticity is potential pseudodensity, and, when making calculations in $(\Phi, \Theta, \mathcal{T})$-space, potential pseudodensity is more convenient. We now define the potential pseudodensity by[1]

$$\sigma^\star = \left(\frac{2\Omega \sin \Phi}{\bar{\zeta}_\theta} \right) \bar{\sigma}, \tag{20.25}$$

so that the potential pseudodensity $\sigma^\star$ is related to the potential vorticity $\hat{P}$ by $\sigma^\star \hat{P} = 2\Omega \sin \Phi$. The potential pseudodensity $\sigma^\star$ is the pseudodensity a parcel would acquire if $\bar{\zeta}_\theta$ were changed to $2\Omega \sin \Phi$ under conservative motion. Because of the simple relation between $\hat{P}$ and $\sigma^\star$, the potential pseudodensity equation is easily obtained from (20.23). It takes the form

$$\frac{\mathcal{D}\sigma^\star}{\mathcal{D}t} + \sigma^\star \left(\frac{\partial(\hat{V} \cos \Phi)}{a \cos \Phi \partial \Phi} + \frac{\partial \hat{\dot{\Theta}}}{\partial \Theta} \right) = 0. \tag{20.26}$$

The flux form of (20.26) is

$$\frac{\partial \sigma^\star}{\partial \mathcal{T}} + \frac{\partial(\sigma^\star \hat{V} \cos \Phi)}{a \cos \Phi \partial \Phi} + \frac{\partial(\sigma^\star \hat{\dot{\Theta}})}{\partial \Theta} = 0. \tag{20.27}$$

The advantage of (20.27) is that, if the source terms $\hat{V}$ and $\hat{\dot{\Theta}}$ are known functions of $(\Phi, \Theta, \mathcal{T})$, one can easily march forward in time using (20.27) only. The problem of the evolution of $\sigma^\star$ has separated from the problem of determining the transverse circulation; no second order elliptic partial differential equation for the transverse circulation needs to be solved each time step. However, when the zonal mean mass field $\bar{p}$ and balanced zonal wind $\bar{u}$ are to be plotted, the $\sigma^\star$ field must be inverted. This problem is discussed below in section 20.4.

Finally, we comment on an apparent limitation in the derivation of the mean flow equations given here. Since the zonal average defined by (20.5) is on an isentropic surface, special care must be used on those isentropic surfaces which intersect the earth's surface. As shown by Andrews (1983), this situation can be handled using the massless layer approach. The basic idea is to continue surface-intersecting isentropes just under the earth's surface and assign to them a pressure equal to the surface pressure. At any horizontal position where two distinct isentropic surfaces run just under the earth's surface (and hence have the same pressure), there is no mass trapped between them, so that $\sigma = 0$ there. Extended definitions of other variables are also required. In addition to such extended definitions, the massless layer approach also requires that the integral on the right hand side of (20.5) be split into intervals of λ where the isentrope is above the earth's surface and intervals where it is below the earth's surface. Since the limits of these integrals depend on (ϕ, θ, t), the $\overline{(\ )}$ operator no longer commutes with $\partial/\partial\phi$, $\partial/\partial\theta$, $\partial/\partial t$. Although the derivations then become more involved, the final equations (20.12)–(20.18) are unmodified except for certain refinements in interpretation.

20.4 Balanced zonal flows

To simplify the zonal mean primitive equation model (20.12)–(20.15) to a balanced model we now assume that the mean zonal flow evolves as a sequence of nearly balanced states. A sufficient condition for the validity of this assumption is that $|\mathcal{G}|$ remains small compared to the magnitude of the pressure gradient and Coriolis terms in (20.13) and that the other forcing terms $\hat{\dot{\theta}}$ and $\mathcal{F}$ have slow enough time scales that significant, zonal mean inertia-gravity waves are not excited, i.e., $|\mathcal{D}\hat{v}/\mathcal{D}t|$ also remains small compared to the magnitude of the pressure gradient and

[1] Note the use of star ($\star$) rather than asterisk ($*$) to avoid confusion with the symbol for deviation from the mass weighted tangential average.

Coriolis terms. We also assume that the right hand side of (20.14) is negligible. Under these conditions (20.13) and (20.14) reduce to

$$\left(2\Omega\sin\phi + \frac{\bar{u}\tan\phi}{a}\right)\bar{u} + \frac{\partial \bar{M}}{a\partial\phi} = 0, \tag{20.28}$$

$$\frac{\partial \bar{M}}{\partial\theta} = \Pi(\bar{p}). \tag{20.29}$$

Using the definitions of $\Pi(\bar{p})$ and $\sigma(\bar{p})$, the set (20.12), (20.15), (20.28) and (20.29) can now be considered as a closed, balanced set in the unknowns $\bar{u}$, $\hat{v}$, $\bar{M}$, $\bar{p}$, all of which are functions of (ϕ, θ, t). However, this is not a convenient set for prediction since (20.12) and (20.15) cannot be used as independent predictors. The prediction of $\bar{u}$ by (20.12) and the prediction of $\bar{\sigma}$ by (20.15) must be consistent with a continuous state of hydrostatic and zonal wind balance, as required by (20.28) and (20.29). This implies that (20.12), (20.15), (20.28) and (20.29) can be combined into a diagnostic equation which can then replace one of the prognostic equations (20.12) or (20.15). To obtain this diagnostic equation, the mass continuity equation (20.15), or equivalently (20.7), is first written in the form

$$\frac{\partial(\bar{\sigma}\hat{v}\cos\phi)}{a\cos\phi\partial\phi} + \frac{\partial(\bar{\sigma}\hat{\dot{\theta}} - \partial\bar{p}/\partial t)}{\partial\theta} = 0, \tag{20.30}$$

which implies that $\bar{\sigma}\hat{v} = -\partial\psi/\partial\theta$ and $\bar{\sigma}\hat{\dot{\theta}} - \partial\bar{p}/\partial t = \partial(\psi\cos\phi)/a\cos\phi\partial\phi$, where ψ is the streamfunction for the meridional circulation. If the first of these is inserted into the zonal momentum equation (20.12), or equivalently (20.9), and the second is multiplied by $\Gamma(\bar{p}) = d\Pi(\bar{p})/d\bar{p} = \kappa\Pi(\bar{p})/\bar{p}$, we obtain

$$\frac{\partial\bar{u}}{\partial t} + \hat{\dot{\theta}}\frac{\partial\bar{u}}{\partial\theta} + \hat{P}\frac{\partial\psi}{\partial\theta} = \mathcal{F}, \tag{20.31}$$

$$\frac{\partial\Pi(\bar{p})}{\partial t} + \hat{\dot{\theta}}\frac{\partial\Pi(\bar{p})}{\partial\theta} + \Gamma\frac{\partial(\psi\cos\phi)}{a\cos\phi\partial\phi} = 0. \tag{20.32}$$

Taking the time derivative of (20.28) and (20.29), and then eliminating $\partial\bar{M}/\partial t$ between the resulting two equations, we obtain

$$\frac{\partial}{\partial\theta}\left(\bar{f}\frac{\partial\bar{u}}{\partial t}\right) + \frac{\partial}{a\partial\phi}\left(\frac{\partial\Pi(\bar{p})}{\partial t}\right) = 0, \tag{20.33}$$

where $\bar{f} = 2\Omega\sin\phi + (2\bar{u}\tan\phi)/a$. Substituting from (20.31) for $\partial\bar{u}/\partial t$ and from (20.32) for $\partial\Pi(\bar{p})/\partial t$, (20.33) becomes

$$\frac{\partial}{a\partial\phi}\left(\Gamma\frac{\partial(\psi\cos\phi)}{a\cos\phi\partial\phi}\right) + \frac{\partial}{\partial\theta}\left(\bar{f}\hat{P}\frac{\partial\psi}{\partial\theta}\right) = \frac{\partial(\Pi(\bar{p}), \hat{\dot{\theta}})}{a\partial(\phi,\theta)} + \frac{\partial(\bar{f}\mathcal{F})}{\partial\theta}. \tag{20.34}$$

This diagnostic equation (often called the Eliassen meridional circulation equation or the Sawyer-Eliassen equation) may be used as a replacement for either (20.12) or (20.15). Then, the balanced system has a single prognostic equation. Since $\Gamma > 0$ everywhere and the usual situation is that $\bar{f}\hat{P} > 0$ almost everywhere[1], (20.34) is a second order elliptic equation for ψ when the forcing functions $\hat{\dot{\theta}}, \mathcal{F}$ are known.

20.5 Invertibility principle

The potential pseudodensity $\sigma^\star$ can be written in Jacobian form using

$$\sigma^\star = \frac{2\Omega\sin\Phi}{\bar{\zeta}_\theta}\bar{\sigma} = -\frac{\partial(\sin\phi)}{\partial(\sin\Phi)}\frac{\partial\bar{p}}{\partial\theta} = -\frac{\partial(\sin\phi,\theta)}{\partial(\sin\Phi,\Theta)}\frac{\partial(\sin\phi,\bar{p})}{\partial(\sin\phi,\theta)} = -\frac{\partial(\sin\phi,\bar{p})}{\partial(\sin\Phi,\Theta)}. \tag{20.35}$$

Introducing the new dependent variable $\bar{\mathcal{M}}$, defined by $\bar{\mathcal{M}} = \bar{M} + \frac{1}{2}\bar{u}^2$, the balance equation (20.28) and the hydrostatic equation (20.29) transform to

$$\left(-2\Omega\sin\Phi\frac{\cos\Phi}{\cos\phi}\bar{u}, \Pi(\bar{p})\right) = \left(\frac{\partial\bar{\mathcal{M}}}{a\partial\Phi}, \frac{\partial\bar{\mathcal{M}}}{\partial\Theta}\right). \tag{20.36}$$

[1] In small regions near the equator, it often happens that $\bar{f}\hat{P} < 0$, due to cross-equatorial movement of air parcels which are conserving their potential vorticity.

Formally, the second part of (20.36) is identical to (20.29) while the first part of (20.36) is simpler than (20.28) in that (20.36) allows only one $\bar{u}$ for a given $\partial\bar{\mathcal{M}}/\partial\Phi$. Using the second part of (20.36), along with the definitions $S = \sin\Phi$ and $s = \sin\phi$, we can now write (20.35) and the first part of (20.36) as

$$\frac{\partial s}{\partial S}\frac{\partial^2\bar{\mathcal{M}}}{\partial\Theta^2} - \frac{\partial s}{\partial\Theta}\frac{\partial^2\bar{\mathcal{M}}}{\partial S\partial\Theta} + \Gamma\sigma^\star = 0, \tag{20.37a}$$

$$2\Omega^2 a^2 S\left(\frac{s^2 - S^2}{1 - s^2}\right) + \frac{\partial\bar{\mathcal{M}}}{\partial S} = 0. \tag{20.37b}$$

Equations (20.37a–b) constitute the desired relation between $\bar{\mathcal{M}}$, s and $\sigma^\star$. If the upper boundary is an isentropic surface with potential temperature Θ_T and the temperature T is specified there (e.g., $T = \text{constant}$ for an isothermal top), the upper boundary condition is simply

$$\frac{\partial\bar{\mathcal{M}}}{\partial\Theta} = \Pi(\bar{p}) \qquad \text{at} \qquad \Theta = \Theta_T. \tag{20.37c}$$

Likewise, if the lower boundary is the isentropic surface with potential temperature $\theta = \theta_B$ and is flat (i.e., $z = 0$ there), then $\bar{M} = \Theta_B\Pi(\bar{p})$ at $\Theta = \Theta_B$. Written in terms of $\bar{\mathcal{M}}$, this lower boundary condition becomes

$$\Theta\frac{\partial\bar{\mathcal{M}}}{\partial\Theta} - \bar{\mathcal{M}} + \frac{\Omega^2 a^2 (s^2 - S^2)^2}{2(1 - s^2)} = 0 \quad \text{at} \quad \Theta = \Theta_B. \tag{20.37d}$$

We can now summarize the results of our analysis as follows. If the time evolution of the $\sigma^\star$ field can be determined from (20.27), we can then solve the diagnostic problem (20.37) for $\bar{\mathcal{M}}$, after which the wind field $\bar{u}$ and the mass field $\bar{\Pi}$ can be determined from (20.36). This is all accomplished in (Φ, Θ) space. The transformation to other representations, e.g., $\bar{u}(\phi, \theta)$ or $\bar{u}(\phi, p)$, is straightforward.

The diagnostic problem (20.37) involves nonlinearity in both the partial differential equation (20.37a), the zonal balance condition (20.37b) and the lower boundary condition (20.37d); also, the factor Γ in (20.37a) depends nonlinearly on $\bar{\mathcal{M}}$ through the hydrostatic relation. However, if we limit our attention to the situation where the potential pseudodensity and the absolute vorticity are positive, the solution of (20.37) is unique. An iterative method must be used for the solution of (20.37).

20.6 Solutions

We now turn to the problem of solving (20.27). For simplicity let us consider the case in which $\hat{V} = 0$ and $\hat{\dot{\theta}}$ is independent of time and is given by $\hat{\dot{\theta}} = Q(S)\sin^2(\pi Z)$, where $Z = (\Theta - \Theta_B)/(\Theta_T - \Theta_B)$ and $Q(S)$ is the latitudinal distribution of the heating. We postpone specification of $Q(S)$ since only the vertical dependence of $\hat{\dot{\theta}}$ is required for our analytic result. Multiplying (20.27) by $\hat{\dot{\theta}}$ we obtain

$$\frac{\partial(\hat{\dot{\theta}}\sigma^\star)}{\partial\tau} + \sin^2(\pi Z)\frac{\partial(\hat{\dot{\theta}}\sigma^\star)}{\partial Z} = 0, \tag{20.38}$$

where $\tau(S) = Q(S)T/(\Theta_T - \Theta_B)$ is the dimensionless "convective clock" time. According to (20.38) the quantity $\hat{\dot{\theta}}\sigma^*$ is constant along each characteristic curve determined from $dZ/\sin^2(\pi Z) = d\tau$. By integration of this equation we can show that the characteristic through the point (Z, τ) intersects the $\tau = 0$ axis at a level $Z_0(Z, \tau)$, determined by $\pi Z_0(Z, \tau) = \cot^{-1}[\pi\tau + \cot(\pi Z)]$. Since $\hat{\dot{\theta}}\sigma^\star$ is constant along each characteristic, its value at (Z, τ) must equal its value at $(Z_0(Z, \tau), 0)$, which results in

$$\sigma^\star(Z, \tau) = \sigma^\star(Z_0(Z, \tau), 0)\frac{\sin^2\{\cot^{-1}[\pi\tau + \cot(\pi Z)]\}}{\sin^2(\pi Z)}. \tag{20.39}$$

Although (20.39) is indeterminant at the boundaries $Z = 0, 1$, use of l'Hopital's rule twice yields $\sigma^\star(Z, \tau) = \sigma^\star(Z_0(Z, \tau), 0)$ at $Z = 0, 1$. Since $Z_0(Z, \tau) \to 0$ as $Z \to 0$ and $Z_0(Z, \tau) \to 1$ as $Z \to 1$, the σ^* field is unmodified at the upper and lower boundaries. The reason for this can be seen by referring back to (20.26) or (20.27) and noting that, for our specified $\dot{\hat{\theta}}$ field, both $\dot{\hat{\theta}}$ and $\partial\dot{\hat{\theta}}/\partial\Theta$ vanish at the boundaries. For the results presented here we have specified the initial $\sigma^\star$ to be a constant, i.e., $\sigma^\star(Z,0) = \sigma_0$, which implies an initial state with no zonal flow.

Equation (20.39) constitutes the analytic solution of the potential pseudodensity equation when the diabatic source has the $\sin^2(\pi Z)$ form. The complete solution $\sigma^\star(S,\Theta,T)$ can be plotted once $Q(S)$, and hence $\tau(S)$, is specified. Since the τ clock runs faster where $Q(S)$ is large, the largest anomalies in the $\sigma^\star$ field will occur in the ITCZ.

For the latitudinal distribution of the heating we now choose the particular form

$$Q(S) = Q_0 4\alpha\pi^{-1/2}\left\{\mathrm{erf}[\alpha(1+S_c)] + \mathrm{erf}[\alpha(1-S_c)]\right\}^{-1}\exp[-\alpha^2(S-S_c)^2], \tag{20.40}$$

where Q_0, α and S_c are specified parameters. By varying the parameters S_c and α we can consider simulated ITCZs centered at different latitudes and with different widths. By integration of (20.40) from the South Pole to the North Pole we can show that $\frac{1}{2}\int Q(S)dS = Q_0$, so that different values of S_c and α all result in the same area averaged heating Q_0. For the results shown here we have chosen $\alpha = 15$ and either $S_c = \sin(10^\circ) \approx 0.174$ or $S_c = \sin(15^\circ) \approx 0.259$. These can be interpreted as rather narrow ITCZs with approximately 85% of their rainfall occurring between 6N and 14N for the $S_c = \sin(10^\circ)$ case or between 11N and 19N for the $S_c = \sin(15^\circ)$ case. Because of the way the product $Q(S)T$ appears in the definition of $\tau(S)$, it is not really necessary to choose Q_0; rather, the solution can simply be obtained for different values of Q_0T. However, for purposes of physical interpretation let us choose $Q_0 = 0.30$ K day^{-1}, along with $\Theta_T = 360$ K and $\Theta_B = 300$ K. Then, the peak heating is $Q(S_c) \approx 5.1$ K day^{-1}, and $T = 3, 6$ days correspond to $Q_0T = 0.9, 1.8$ K, or $\tau(S_c) \approx 0.26, 0.51$.

For the case of an ITCZ at 10°N the fields of $\sigma^\star(\phi,\theta)$, $P(\phi,\theta)$, $u(\phi,\theta)$ and $p(\phi,\theta)$ at 3 and 6 days are shown in Figs. 20.1 and 20.2 (JAS, **48**, 1493–1509). The $\sigma^\star$ field has been normalized by $\sigma_0 = 1.458$ kPa K^{-1} and the $\hat{P}$ field by $2\Omega/\sigma_0$. In the ITCZ, a region of small potential pseudodensity develops at lower levels and a region of large potential pseudodensity at upper levels. Due to vertical advection in the ITCZ, the lower tropospheric minimum in $\sigma^\star$ begins to form an indentation on the upper tropospheric maximum in $\sigma^\star$. This same process occurs in a more extreme form in the development of a tropical cyclone. The solution of the invertibility principle results in low level zonal flows, which are easterly except in a band that runs between a latitude just north of the equator and a latitude near the center of the ITCZ. At upper levels the zonal flow is westerly except in a band that runs between a latitude just south of the equator and a latitude near the center of the ITCZ. As the $\sigma^\star$ and P anomalies become larger, the associated zonal flows also become larger. The isolines of pressure in the bottom panels of Figs. 20.1 and 20.2 reveal only small adjustments in the mass field, with a slight stabilization at lower levels in the ITCZ and a slight destabilization aloft.

Perhaps the most striking result seen in Figs. 20.1 and 20.2 is that a narrow potential pseudodensity or potential vorticity anomaly produced in just a few days by convection in the ITCZ can result in significant zonal winds throughout the entire tropical and subtropical region. This result is related to the meridional parcel displacements forced by the convection. Since Φ is a conservative quantity and $\dot{\hat{\theta}}$ is known, and since the actual latitude $\phi(\Phi,\Theta)$ is part of the solution of the invertibility problem, meridional parcel displacements or trajectories are easy to construct. Two sets of such trajectories from the initial time to 3 days and from 3 to 6 days are shown in Fig. 20.3, along with the $\dot{\hat{\theta}}$ field. Away from the ITCZ, $\dot{\hat{\theta}} = 0$ and parcel trajectories are along isentropic surfaces. In a lower tropospheric layer bounded by two isentropes, mass is removed in the ITCZ, and there is a shift in parcel positions toward the ITCZ. The largest shifts are on the cross-equatorial side, because $\bar{f}\hat{P}$ is smallest there. Corresponding shifts away from the ITCZ occur in an upper tropospheric layer bounded by two isentropes. As the heating proceeds, $\bar{f}\hat{P}$ becomes larger in the lower troposphere near the ITCZ. This increasing resistance to motion along isentropic surfaces, coupled with the fixed $\dot{\hat{\theta}}$ field, causes the depth of the ITCZ inflow to deepen with time.

The anisotropic response or enhancement of the cross-equatorial Hadley cell has interesting effects on the potential vorticity field. To see this, consider the -0.1 and 0.4 potential vorticity lines in Figs. 20.1 and 20.2. These $\hat{P}$ lines mark chains of fluid particles beginning approximately equal distances from the ITCZ. At 6 days the -0.1 line is more distorted than the 0.4 line. This is a direct result of the fact that the meridional circulation associated with the cross-equatorial Hadley cell is more intense than the meridional circulation associated with the Hadley cell north of the ITCZ. The $\hat{P} = 0$ curve marks the chain of fluid particles which started at rest on the equator. Regardless of the hemisphere into which these particles move, they must acquire a westerly flow, since they move closer to the axis of the earth's rotation. Thus, the $\hat{P} = 0$ line bends more than the $u = 0$ line, so that it lies in the lower tropospheric westerlies north of the equator and the upper tropospheric westerlies south of the equator.

The convective modification of the PV field occurs within a background state that has a northward increase of PV. As convection continues, the gradient of PV becomes locally reversed in the lower troposphere poleward of the ITCZ and in the upper troposphere equatorward of the ITCZ. These regions of reversed isentropic poleward gradient of PV are indicated by stippling in Figs. 20.1 and 20.2. Such features develop quickly and satisfy the necessary condition for combined barotropic-baroclinic instability. Thus, it would appear that ITCZ convection alone can lead to the generation of unstable zonal flows. This may be the cause of periodic breakdowns of the ITCZ.

Results at 6 days for an ITCZ located at $15°$N are shown in Fig. 20.4. Comparing Fig. 20.4 with Fig. 20.2 we note that, except for the latitudinal shift, the $\sigma^\star$ fields are essentially identical. However, the potential vorticity, zonal wind and mass fields are different, with the ITCZ at $15°$N producing a PV anomaly, neighboring zonal winds and isobaric surface deviations considerably larger than those produced by the ITCZ at $10°$N. These differences can be interpreted as follows. Since $D\sigma^\star/Dt = -\sigma^\star(\partial\dot{\hat{\theta}}/\partial\Theta)$ and the initial $\sigma^\star$ is constant, the time evolution of σ^* for ITCZs at different latitudes is essentially identical except for the meridional shift. Since $D\hat{P}/Dt = \hat{P}(\partial\dot{\hat{\theta}}/\partial\Theta)$ and the initial $\hat{P}$ increases to the north, the material rate of change of $\hat{P}$ is larger for an ITCZ at $15°$N. An alternate interpretaion is that, since $\hat{P} = (2\Omega \sin\Phi)/\sigma^\star$, identical $\sigma^\star$ anomalies shifted from $10°$N to $15°$N result in $\hat{P}$ anomalies which are approximately 50% larger for the ITCZ at $15°$N.

Problems

1. Derive (20.12) from (20.9).
2. Derive (20.13) from (20.11) and (20.7).
3. Derive (20.19) from (20.9). Then combine (20.19) with (20.15) to obtain (20.20).
4. Derive (20.33) from (20.28) and (20.29). Then combine (20.31), (20.32) and (20.33) to obtain the Eliassen equation (20.34).
5. Show by direct substitution that (20.39) is a solution of (20.38).

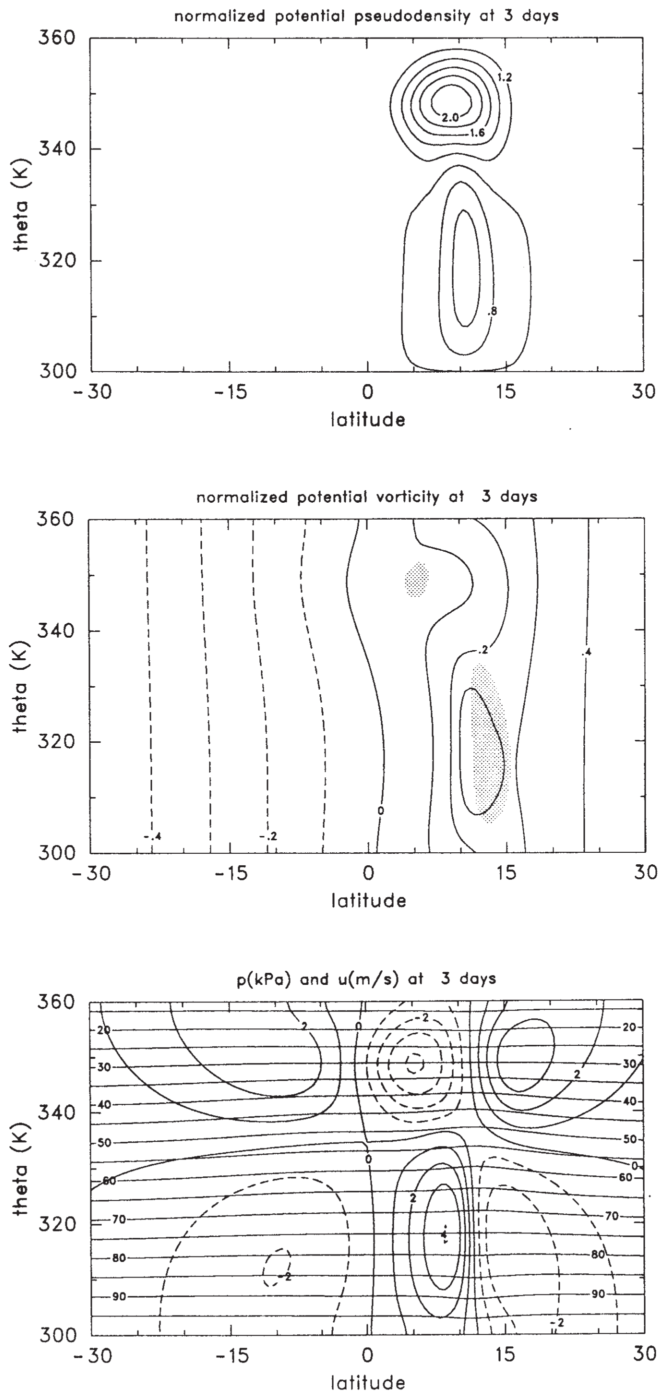

Figure 20.1: Results at $T = 3$ days for an ITCZ located at 10N. The upper panel shows isolines of $\sigma^{\star}/\sigma_0$ (i.e., potential pseudodensity measured in units of σ_0) in (ϕ, θ)-space. Note that the convection in the ITCZ generates a lower tropospheric region of low potential pseudodensity and an upper tropospheric region of high potential pseudodensity. The middle panel shows isolines of $P\sigma_0/(2\Omega)$ (i.e., potential vorticity measured in units of $2\Omega/\sigma_0$). The stippling indicates regions where the poleward isentropic gradient of potential vorticity is reversed. The bottom panel shows pressure (nearly horizontal lines) in kPa and zonal balanced wind in m s^{-1}. Solid wind contours indicate westerly flow, dashed contours easterly flow, with a contour interval of 1 m s^{-1}. These wind and mass fields are in (ϕ, θ)-space and are associated with the potential pseudodensity and potential vorticity fields shown in the top two panels.

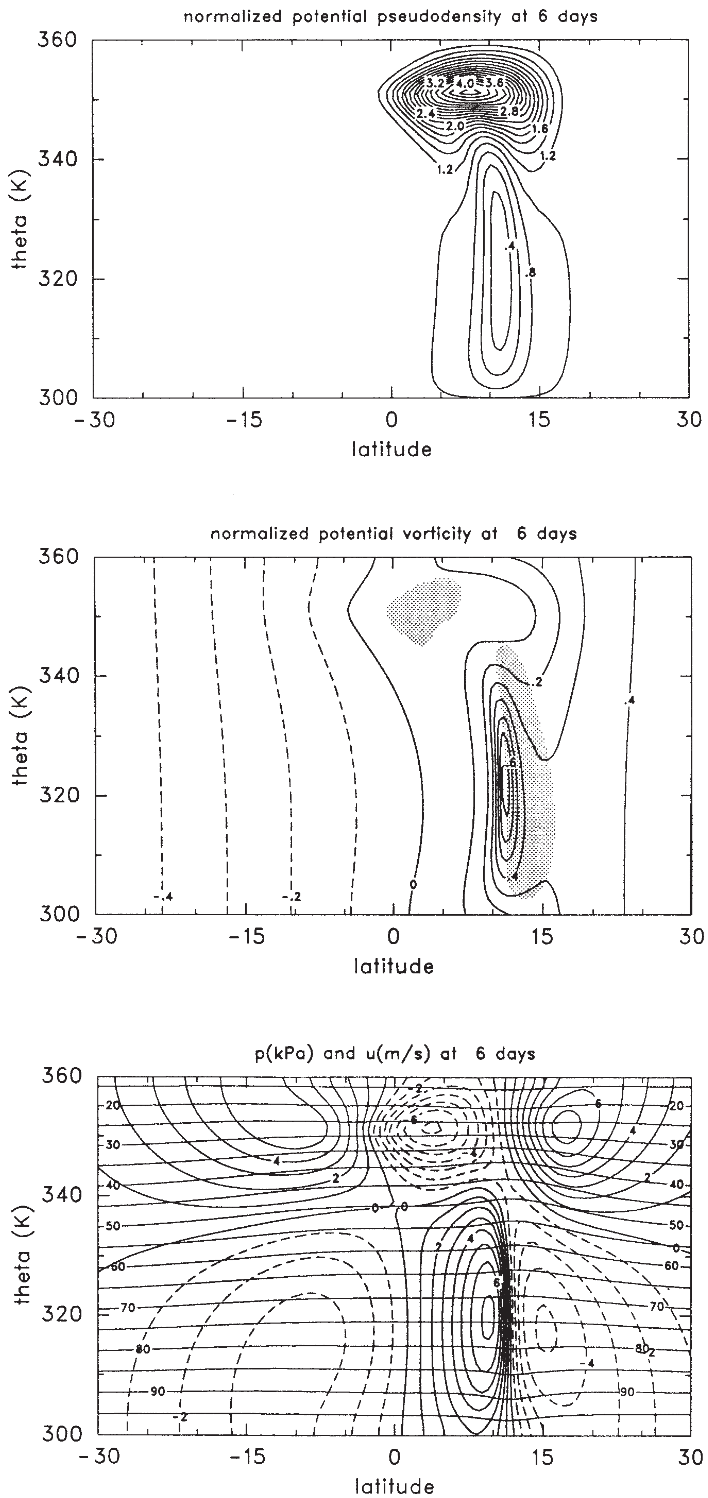

Figure 20.2: Results at $T = 6$ days for an ITCZ located at 10N.

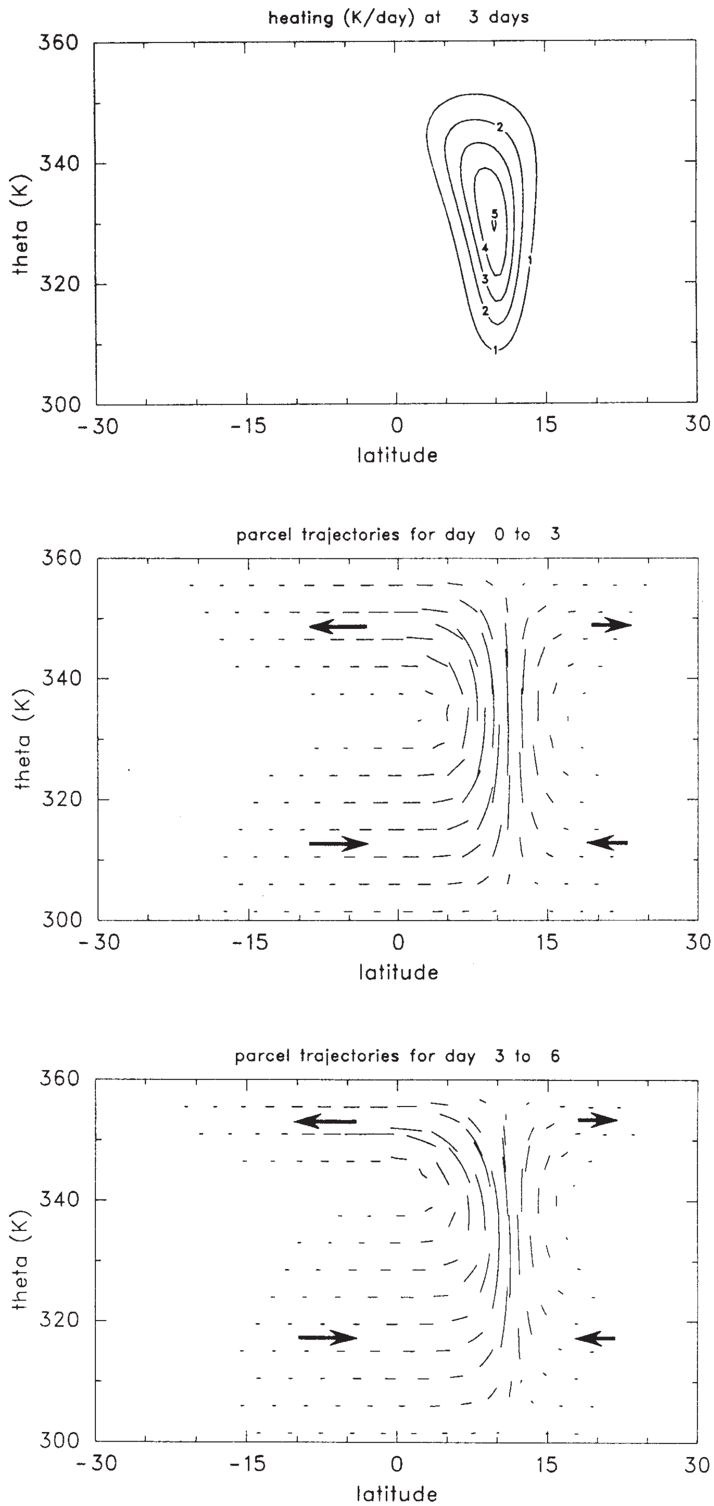

Figure 20.3: The upper panel shows the heating function $\hat{\dot{\theta}}(\phi, \theta)$ in K day^{-1} at 3 days. The distortion of the heating function from a true Gaussian function results from the transformation to actual latitude ϕ. The other two panels show parcel trajectories from the initial time to 3 days and from 3 days to 6 days. The cross-equatorial cell is more intense because the inertial stability $\bar{f}\hat{P}$ in (20.34) is smaller near the equator. Thus, air parcels near the equator encounter the least resistance to "horizontal" movement along isentropic surfaces.

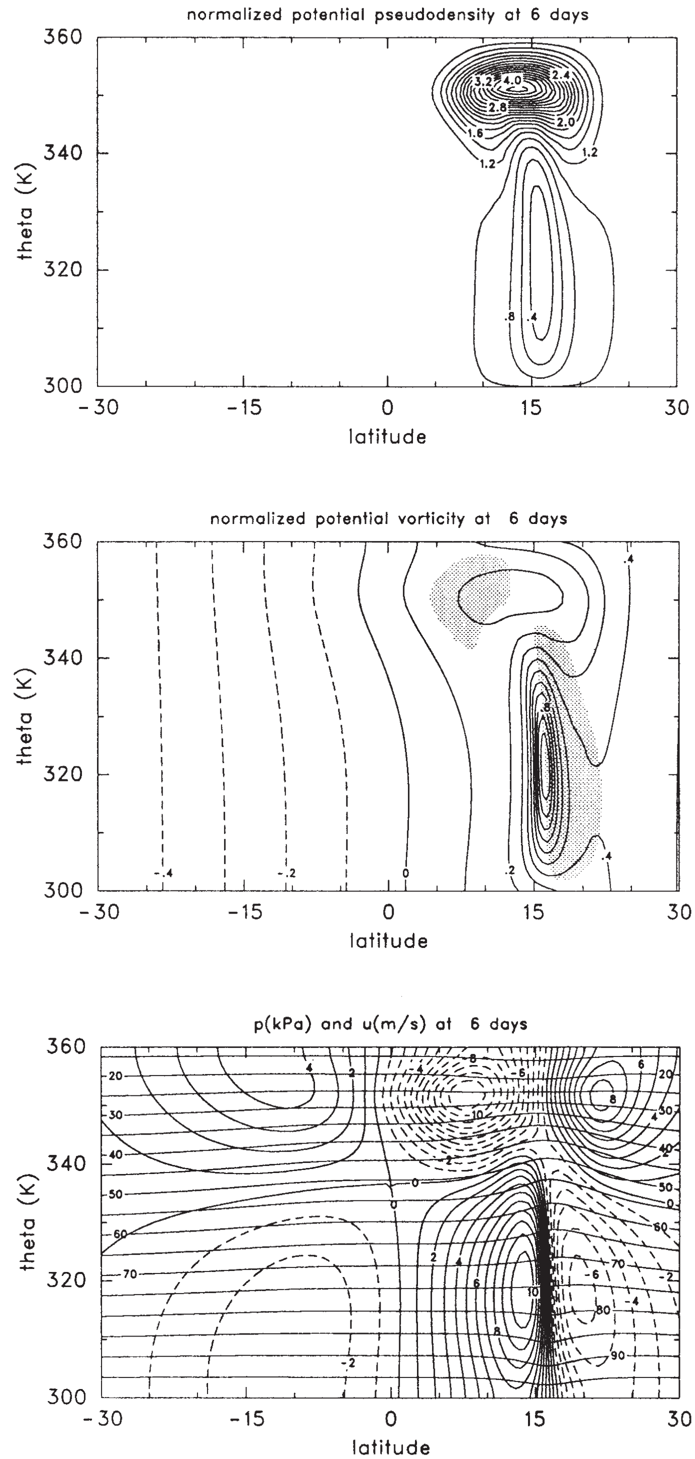

Figure 20.4: Results at $T = 6$ days for an ITCZ located at 15N.